A fast marching method based back projection algorithm for photoacoustic tomography in heterogeneous media

Tianren Wang and Yun Jing

Abstract

This paper presents a numerical study on a fast marching method based back projection reconstruction algorithm for photoacoustic tomography in heterogeneous media. Transcranial imaging is used here as a case study. To correct for the phase aberration from the heterogeneity (i.e., skull), the fast marching method is adopted to compute the phase delay based on the known speed of sound distribution, and the phase delay is taken into account by the back projection algorithm for more accurate reconstructions. It is shown that the proposed algorithm is more accurate than the conventional back projection algorithm, but slightly less accurate than the time reversal algorithm particularly in the area close to the skull. However, the image reconstruction time for the proposed algorithm can be as little as 124 ms when implemented by a GPU (512 sensors, 21323 pixels reconstructed), which is two orders of magnitude faster than the time reversal reconstruction. The proposed algorithm, therefore, not only corrects for the phase aberration, but can be also potentially implemented in a real-time manner.

Index Terms

Fast marching method, back projection, transcranial, heterogeneous media

I. INTRODUCTION

Various algorithms with different experimental configurations have been proposed [1][2][3][4] to reconstruct the photo-acoustic tomography (PAT) image. Back projection (BP) is the most commonly adopted one [5] due to its simplification and universality to a wide range of sensor configurations. The BP is based on the assumption that the speed of sound distribution is relatively constant. This is typically considered valid for soft tissue. For heterogeneous media, such as for brain cerebral vascular imaging, however, traditional BP algorithm results in poor reconstruction images. This is mainly because of the presence of the skull, of which the acoustic properties differ dramatically from the surrounding medium. For example, the speed of sound in the skull is $2200 - 3000$ m/sec while the speed

T. Wang and Y. Jing are with the Department of Mechanical and Aerospace Engineering, North Carolina State University, Raleigh, NC 27695 (e-mail: yjing2@ncsu.edu)

of sound in the brain tissue is around 1540 m/sec [6]. Such a strong heterogeneity violates the assumption of the back projection algorithm. On the other hand, even for weakly heterogeneous media, BP algorithm is shown to be suboptimal [7]. Some modified BP methods have been proposed to mitigate the effect of phase aberration, such as using a half-time algorithm [8]. A ray-tracing method can be incorporated to correct for the phase distortion [6]. Nevertheless, it has been so far limited to simple, three-layered geometries.

Time reversal reconstruction has become progressively popular in recent years with the development of high-performance computers. In time reversal reconstruction, all the acoustic transducers are considered as sources and the received acoustic signals are propagated backwards in a time-reversed manner [9]. Time-reversal reconstruction arrives at better results as it takes full advantages of the wave equation. However, the time reversal reconstruction imaging method is very time consuming because the full wave equation is solved in the time-domain by either the finite-difference time-domain (FDTD) method or the k-space method, therefore is less applicable for real-time imaging. Iterative image reconstruction algorithms suffer from the similar drawback in terms of image reconstruction speed [7][10]. Although PAT images can be processed off-line, real-time PAT provides unique opportunities, such as detection and interpretation of brain activation patterns for online decision making in neuroscience and clinical applications (e.g., lie detection and pre-surgical mapping [11]). It also allows for real-time monitoring of interventional procedures and drug delivery.

The goal of this study is to investigate a fast marching method (FMM) based, non-iterative BP algorithm, which can be potentially realized in real-time. The FMM calculates the arrival time from a pixel (to be imaged) to all sensors in order to account for the phase delay due to the heterogeneity, provided that the speed of sound distribution is known. The phase delay can be simply included in the BP algorithm. Numerical simulations will be presented for PAT brain cerebral vascular imaging to demonstrate the effectiveness of the proposed algorithm. The paper is structured as follows: In Sec. II the wave propagation model and FMM are briefly revisited; the FMM based BP algorithm for PAT in heterogeneous media is then introduced. Section III discusses simulation results of photoacoustic transcranial imaging using the proposed and other existing methods. Section IV discusses and concludes the paper.

II. Algorithm

A. Wave propagation

1) Photo-acoustic wave equation: Because the PAT initial pressure is typically on the order of 10 kPa [2], the governing equation comprises the linearized equations of mass, continuity, and pressure:

$$\frac{\partial}{\partial t}u(x,t) = -\frac{1}{\rho_0(x)}\nabla p(x,t) \tag{1}$$

$$\frac{\partial}{\partial t}\rho(x,t) = -\rho_0(x)\nabla u(x,t) \tag{2}$$

$$p(x,t) = c(x)^2\rho(x,t) \tag{3}$$

with the initial conditions being:

$$p(x,t)|_{t=0} = p_0(x), u(x,t)|_{t_0} = 0, \tag{4}$$

where p is the acoustic pressure at time t with location x, c is the sound speed, u is the acoustic particle velocity, ρ is the acoustic density and ρ_0 is the ambient density. Even though shear waves could be generated with the signal propagates from brain tissue to the skull, it was not considered in this study because 1: shear waves are strongly attenuated when propagating in the skull [12]; 2: the sound speed of shear waves in the skull is around 1500 m/sec which is much slower than the sound speed of the longitudinal wave [12] , so it will take longer time for the shear wave to arrive at the sensor. The center frequencies are also distinct from shear and longitudinal waves [6]. The time difference and frequency difference make it easy to discriminate the shear wave from the longitudinal wave.

2) K-space method: Previous studies [2][13] have shown that the k-space algorithm is accurate and efficient for solving the wave equation. In this study, a k-space method based open source software K-WAVE [2] was adopted to simulate the PAT ultrasound signal. Details of implementation of the k-space algorithm can be found at [2].

B. Fast marching method

It has been shown [14][15] that FMM is an effective method to compute the evolution of wave fronts governed by the Eikonal equation, which is a high frequency approximation of the wave equation (i.e., the scale of variation of the speed of sound is assumed to be much greater than the acoustic wavelength [16]) and reads

$$|\nabla T|^2 = 1/c^2, \tag{5}$$

where T is the wave front arrival time and c is the sound speed at a given location. For a 2D situation, starting with an initial condition, the neighboring point with the shortest arrival time is calculated. This repeats recursively until all the points in the region are visited. A second-order approximation was used to calculate the arrival time [15].

$$\frac{\partial T}{\partial x} = \frac{3T(x,y) - 4T(x-1,y) + T(x-2,y)}{2}. \tag{6}$$

The proposed BP method makes use of the arrival times/time-of-flight (TOF) from all pixels to each of the sensor point. This can be achieved by assigning each pixel point as a point source, and calculates the corresponding TOF map. However, as can be seen in the numerical simulation section, there are typically a lot more pixel points than sensor points. We therefore assigned each sensor point as a point source, and calculated the TOF at all pixel points of interest, since the ray path is reversible. The TOF can be integrated into the BP method for reconstruction as shown below.

C. FMM based back projection

BP, which is also known as the Kirchhoff migration, has been widely used in seismology imaging [17]. In the past decades, back projection and its various modified version have been applied to biomedical imaging applications [5] . A recent study on breast ultrasound imaging shows that the Kirchhoff migration can be improved by taking the arrival times in a heterogeneous medium into account [18].

In that paper, the TOF has to be calculated for a ray path from the source to the pixel, and then to the sensor. In PAT, only one-way propagations are present. The modified BP in combination with the FMM method is shown below as:

$$P(\overrightarrow{r_j}) = \sum_{i=\text{receiver index}} [p_i(t_{i,j}) - t_{i,j} \frac{\partial p_i(t_{i,j})}{\partial t}] \tag{7}$$

where $P(\overrightarrow{r_j})$ is the pixel magnitude at the jth location (at $\overrightarrow{r_j}$) in the reconstruction area. $p_i(t_{i,j})$ is the ultrasound pressure signal received at the ith sensor location. $t_{i,j}$ is the TOF from reconstruction location $\overrightarrow{r_j}$ to the ith transducer location calculated from the FMM. In the conventional BP algorithm, $t_{i,j}$ is calculated analytically by assuming a constant speed. It is noted that, Eq. 7 can be viewed as an approximation to the exact BP algorithm [5]. It assumes a circular scanning geometry and that the scanning radius is considerably larger than the region of interest [19].

III. NUMERICAL SIMULATION

In this section, 2D numerical simulations were implemented to validate the proposed FMM based BP algorithm. A rhesus macaque monkey skull was chosen for the numerical simulation. The acoustic properties (speed of sound, density and attenuation) of the monkey skull were derived from its CT scan based on the method described in [20] (Fig. 1). The sound speed of the brain tissue was 1540 m/sec and the mean sound speed of skull was around 2450 m/sec. The absorption was assumed to be linearly frequency dependent and the attenuation of the brain tissue was set to be 0.65 dB/cm/MHz. A ring array of 512 sensors was positioned around the skull to receive the acoustic signals (Fig. 3 (a)). These sensors were assumed to have flat frequency response for simplification. For the forward photoacoustic simulation carried out by K-WAVE, the spatial resolution was set to be 0.195 mm. A majority of the broadband photoacoustic signal energy resides at frequencies less than 1 MHz [21], and the resolution was chosen because it is about $1/8$ of the wavelength at 1 MHz and was considered sufficiently small. The Courant-Friedriches-Lewy (CFL) number was 0.03. This small CFL number was chosen to maintain the stability of the k-space algorithm under extremely large absorption in the skull. The end time for both forward and backward wave propagation was $1.5 \times d/c_0$, where d is the diameter of the ring array and c_0 is the background speed of sound. Results did not change significantly when using an end time greater than this. Figure 2 presents the TOF map acquired from FMM due to a point source at an arbitrary sensor point. The arrival time distribution within the skull region will be used for correcting the phase delay in the BP algorithm. In this study, FMM was applied to

the speed of sound distribution derived from the CT scan. A recent study also used CT scans of skulls for phase correction, but the reconstruction was based on the time reversal reconstruction [21].
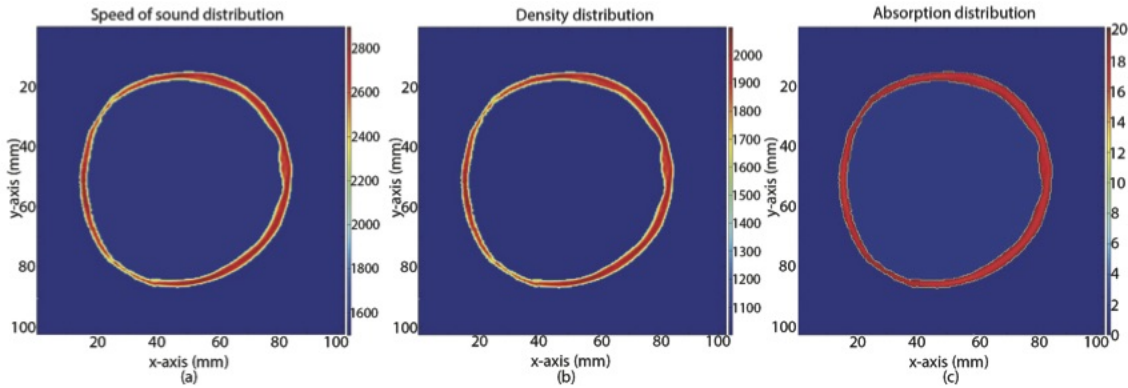

Fig. 1.   (Color online) Acoustic properties derived from the CT scan for a monkey skull.(a) speed of sound distribution (m/s). (b) density distribution (kg/m^3). (c) absorption distribution (dB/cm/MHz).

An image with the same resolution as in the forward simulation was reconstructed using the FMM based BP method, as shown in Fig.3 (b). For computational efficiency purpose, the reconstructions were only implemented for the area within the skull, i.e., 85291 pixels in total were reconstructed. The conventional BP reconstruction without phase correction and the time reversal reconstruction were also implemented for comparison. For the conventional BP, a constant speed of sound at 1560 m/s was used and was determined by an automatic sound speed selection algorithm [22]. The results are shown in Fig. 3 (c) and (d), respectively. The image quality resulted from the FMM based BP method (Fig. 3 (b)) is considerably better than that of the conventional BP (Fig. 3 (c)), which was distorted and blurred. As the phase correction step (FMM) in the proposed method only needs to be calculated during the off-line process once (the entire FMM computation took 184.28 seconds in this study), the online computation time of the proposed method is the same as the conventional BP. It is noted that the off-line process needs to be repeated though if the sensor positions are changed. To achieve efficient computation, the reconstruction algorithm was implemented in GPU[23] using an NVIDIA Tesla C2075 with 6GB of memory and 14 multiprocessors with computation capability 2.0. The GPU variable grid $dim3$ was set to be $(32, 2, 1)$ and the GPU variable thread $dim3$ was set to be $(32, 32, 1)$. The computation time, including transferring data from CPU memory to GPU memory, image reconstruction, and transferring data back to CPU, was 241.83 ms in total, indicating almost 4 frames per second (fps). This is about three orders of magnitude faster than on an Intel Xeon E5620 CPU. A similar amount of computational speed-up using GPUs was also recently reported [23]. The processing time can be further reduced to 123.79 ms if the spatial resolution was changed from 0.195 mm to 0.39 mm (21323 pixels) without compromising the accuracy. For comparison, the time reversal reconstruction was also implemented in GPU with the CFL number set to 0.24 and a spatial resolution of 0.195 mm. A larger CFL number was used in the backward propagation because the attenuation was not considered. The computation time was 43.89 seconds. It is worth pointing out

that with the FMM based BP, a specific region of interest can be selected for reconstruction to further reduce the reconstruction time. This is in general not possible for the time reversal reconstruction.
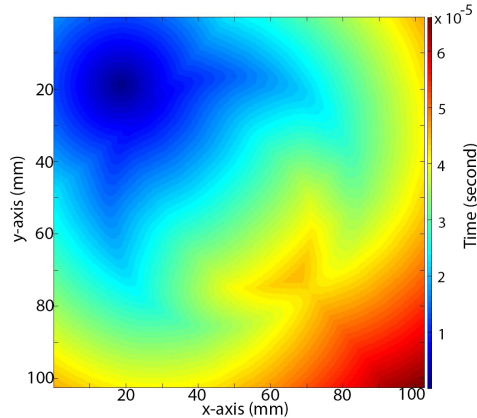

Fig. 2. (Color online) Arrival times calculated by FMM when a point source is assigned at a sensor located at (18.36 mm, 18.36 mm).

The result of the time reversal method, as shown in Fig. 3 (d), has the best accuracy as expected. Comparing Fig. 3 (b) to (d), it is found that the main difference is the region close to the skull, which is not well reconstructed by the modified BP. This is consistent with the conclusion of [6]: the region close to the skull is more susceptible to the phase aberration from the skull. Even though the result from the time reversal reconstruction is less distorted than the result of the proposed method, the time reversal method is significantly more time consuming as demonstrated above, therefore is not feasible for real-time imaging. Close-up comparisons are also provided in Fig. 4, where the center of the vessel is shown. It should be borne in mind that, photo-acoustic waves in 2D are not compactly supported. This means that time reversal reconstruction for PAT is not exact in 2D. However, 3D simulations are extremely time- and memory-consuming and therefore were not investigated.

Finally, we investigated the robustness of our algorithm against errors in the skull sound speed. Similar to a previous study [10], 1.7% (with respect to maximum value) uncorrelated Gaussian noise with mean value of 1.7% of the maximum value was added to the speed of sound maps. The density errors were not studied as it should not affect the BP algorithm. Results are shown in Fig. 5 and no significant changes are observed. The width of the vessel, however, does seem to be overestimated when speed of sound errors are present. Comparing Fig. 5 (a) to Fig.3 (c), the modified BP algorithm is still more accurate than the original BP using a constant speed of sound. For example, the top portion of the vessel seems to split into two parts in Fig. 3 (c). This artifact is not seen in Fig. 5 (a). In this study, the monkey skull was relatively rounded. We expect the conventional BP to be even more inaccurate when the skull has a less regular shape (e.g., more or less elliptical, such as for human skulls) and ring array is used again. This is because the phase delays in this case become more non-uniform with regard to each sensor, therefore can not be easily compensated using a constant phase correction.
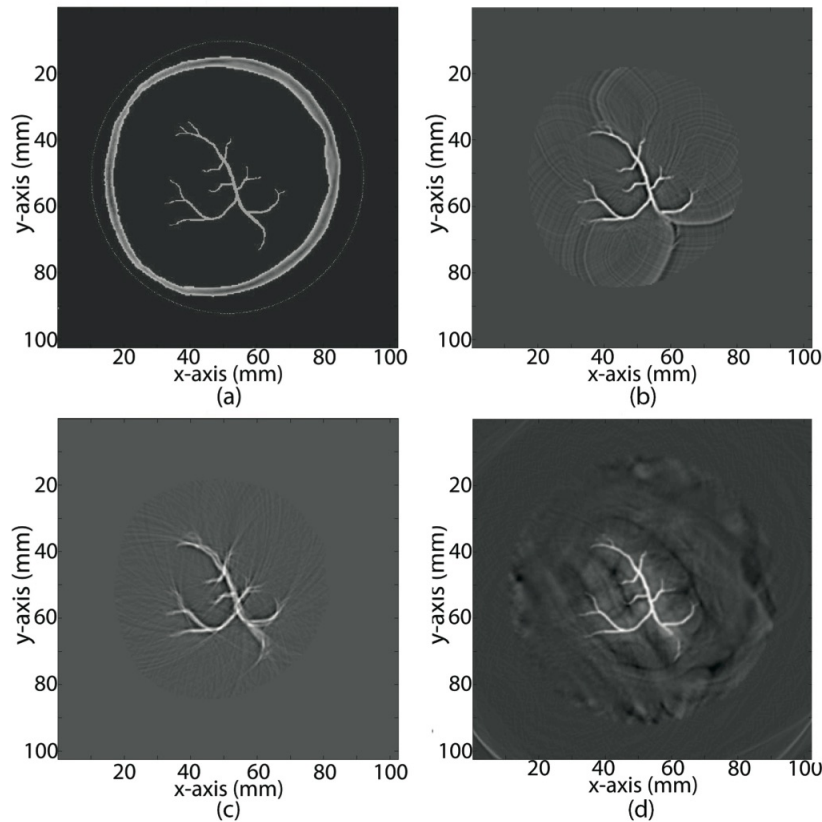
Fig. 3. (a) Monkey brain model. The white dots encircling the skull show the locations of the 512 sensors. The cerebral vascular is the object to be imaged. Reconstructed images using different algorithms are compared. (b) FMM based BP reconstruction; (c) conventional BP using the optimal background speed of sound; (d) time reversal reconstruction.

IV. CONCLUSION

This paper demonstrates a method for correcting the phase aberration in PAT imaging in heterogeneous media. Even though the skull was assumed to be the heterogeneity in this study, the proposed algorithm can be applied to general tissue heterogeneities, such as in breasts, kidneys, etc. The conventional BP method was modified by taking the delayed time/phase into account, which was conveniently computed by the FMM. Improvement over conventional BP algorithm in terms of reconstructed images was achieved. Compared to the most accurate time reversal reconstruction, the proposed algorithm was two orders of magnitude faster, and at the curate stage can be implemented in quasi-real-time. However, we envision that truly real-time 2D PAT reconstruction is possible in the near future with the fast development of GPU technology. We also note that in practice, BP in fact could have a higher computational complexity than time reversal reconstruction [24]. In this study, BP was shown to be faster because it can be significantly accelerated utilizing the superior parallel computing power of GPUs [23]. It is not the case, though, for time reversal reconstruction, since the solution at each time step is dependent on the previous one. In other words, all the time steps have to be implemented sequentially as opposed to in parallel.
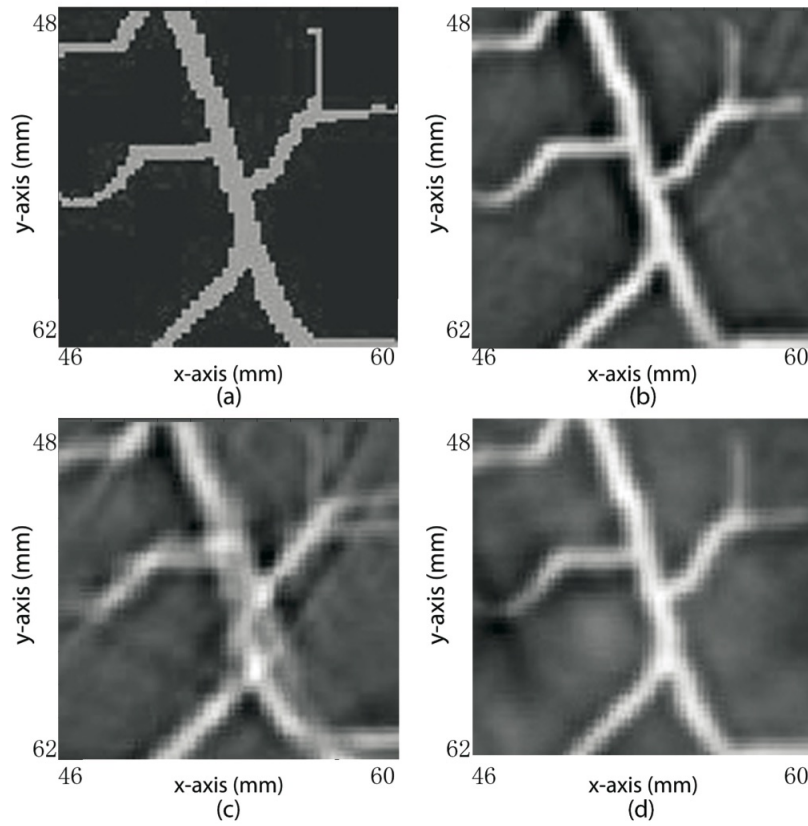
Fig. 4. Close-up comparison between different algorithms. The center of the vessel is shown. (a) True image; (b) FMM based BP reconstruction; (c) conventional BP using the optimal background speed of sound; (d) time reversal reconstruction.
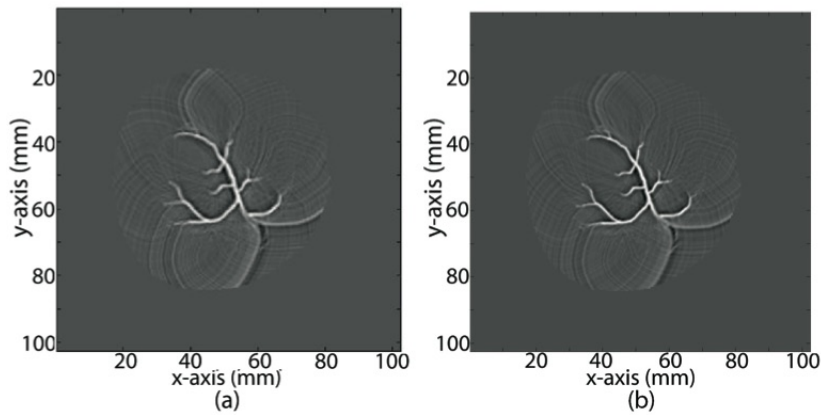

Fig. 5. (a) Reconstructed image with the speed of sound error. (b) Reconstructed image without the speed of sound error.

Because the modified BP algorithm has the same on-line computation speed to the original BP algorithm, we expect such an algorithm, once implemented for 3D image reconstruction, could be completed on the order of

seconds using currently existing GPUs [23].

As the current study is a proof-of-concept numerical study, we intend to implement the algorithm proposed here on ex vivo monkey skulls to further evaluate the potential of the approach as a future study. In this way, dispersion, shear waves, and out-of plane refraction could be naturally taken into account.

References

[1] M. Xu, Y. Xu, and L. V. Wang, "Time-domain reconstruction algorithms and numerical simulations for thermoacoustic tomography in various geometries." *IEEE Trans. Biomed. Engineering*, vol. 50, no. 9, pp. 1086–1099, 2003.

[2] B. E. Treeby and B. T. Cox, "k-wave: Matlab toolbox for the simulation and reconstruction of photoacoustic wave-fields." *J. Biomed. Opt.*, vol. 15, p. 021314, 2010.

[3] C. Zhang, C. Li, and L. V. Wang, "Fast and robust deconvolution-based image reconstruction for photoacoustic tomography in circular geometry: experimental validation." *IEEE Photonics J.*, pp. 57–66, 2010.

[4] J. Niederhauser, M. Jaeger, R. Lemor, P. Weber, and M. Frenz, "Combined ultrasound and optoacoustic system for real-time high-contrast vascular imaging in vivo." *Medical Imaging, IEEE Transactions on*, vol. 24, no. 4, pp. 436–440, 2005.

[5] M. Xu and L. V. Wang, "Universal back-projection algorithm for photoacoustic computed tomography." *Phys. Rev. E*, vol. 71, p. 016706, Jan 2005.

[6] X. Jin, C. Li, and L. V. Wang, "Effects of acoustic heterogeneities on transcranial brain imaging with microwave-induced thermoacoustic tomography." *Medical Physics*, vol. 35, pp. 3205–3214, 2008.

[7] J. Jose, R. G. H. Willemink, W. Steenbergen, C. H. Slump, T. G. van Leeuwen, and S. Manohar, "Speed-of-sound compensated photoacoustic tomography for accurate imaging." *Med Phys.*, vol. 39, no. 12, pp. 7262–7271, 2012.

[8] M. Anastasio, J. Zhang, X. Pan, Y. Zou, G. Ku, and L. V. Wang, "Half-time image reconstruction in thermoacoustic tomography." *Medical Imaging, IEEE Transactions on*, vol. 24, no. 2, pp. 199–210, 2005.

[9] Z. Liu, L. Liu, Y. Xu, and L. V.Wang, "Transcranial thermoacoustic tomography: A comparison of two imaging algorithms." *IEEE transactions on medical imaging*, vol. 32, pp. 289–294, 2013.

[10] C. Huang, K. Wang, L. Nie, L. V. Wang, and M. A. Anastasio, "Full-wave iterative image reconstruction in photoacoustic tomography with acoustically inhomogeneous media." *medical imaging, IEEE transactions on*, vol. 32, pp. 1097–1110, Mar 2013.

[11] J. Lachaux, K. Jerbi, O. Bertrand, L. Minotti, D. Hoffmann, B. Schoendorff, and P. Kahane, "A blueprint for real-time functional mapping via human intracranial recordings," *PLoS One.*, vol. 2, p. e1094, 2007.

[12] P. White, G. Clement, and K. Hynynen, "Longitudinal and shear mode ultrasound propagation in human skull bone." *Ultrasound Med Biol*, vol. 32, no. 7, pp. 1085–1096, 2006.

[13] Y. Jing, F. C. Meral, and G. T. Clement, "Time-reversal transcranial ultrasound beam focusing using a k-space method." *Physics in Medicine and Biology*, vol. 57, pp. 901–917, 2012.

[14] T. Wang and Y. Jing, "Transcranial ultrasound imaging with speed of sound-based phase correction: a numerical study." *Physics in Medicine and Biology*, vol. 58, no. 19, pp. 6663–6681, 2013.

[15] J. A. Sethian and A. Vladimirsky, "Fast methods for the eikonal and related hamilton jacobi equations on unstructured meshes." *Proceedings of The National Academy of Sciences*, vol. 97, pp. 5699–5703, 2000.

[16] D. Modgil, M. A. Anastasio, and P. J. L. Rivire, "Image reconstruction in photoacoustic tomography with variable speed of sound using a higher-order geometrical acoustics approximation." *J. Biomed. Opt.*, vol. 15, p. 021308, 2009.

[17] W. Schneider, "Integral formulation for migration in two and three dimensions." *Geophysics*, vol. 43, pp. 49–76, 1978.

[18] S. Schmidt, N. Duric, C. Li, O. Roy, and Z.-F. Huang, "Modification of kirchhoff migration with variable sound speed and attenuation for acoustic imaging of media and application to tomographic imaging of the breast." *Medical Physics*, vol. 38, no. 2, pp. 998–1007, 2011.

[19] X. Dean-Ben, R. Ma, D. Razansky, and V. Ntziachristos, "Statistical approach for optoacoustic image reconstruction in the presence of strong acoustic heterogeneities," *IEEE Transactions on Medical Imaging*, vol. 30, pp. 401–408, 2011.

[20] J. Aubry, M. Tanter, M. Pernot, J. Thomas, and M. Fink, "Experimental demonstration of noninvasive transskull adaptive focusing based on prior computed tomography scans." *J Acoust Soc Am*, vol. 113, pp. 84–93, 2003.

[21] C. Huang, L. Nie, R. W. Schoonover, Z. Guo, C. O. Schirra, M. A. Anastasio, and L. V. Wang, "Aberration correction for transcranial photoacoustic tomography of primates employing adjunct image data." *Journal of Biomedical Optics*, vol. 17, no. 6, p. 066016, 2012.

[22] B. E. Treeby, T. Varslot, E. Z. Zhang, J. G. Laufer, and P. C. Beard, "Automatic sound speed selection in photoacoustic image reconstruction using an autofocus approach." *J. Biomed. Opt.*, vol. 16, p. 090501, 2011.

[23] K. Wang, C. Huang, Y.-J. Kao, C.-Y. Chou, A. A. Oraevsky, and M. A. Anastasio, "Accelerating image reconstruction in three-dimensional optoacoustic tomography on graphics processing units." *Medical Physics*, vol. 40, no. 2, p. 023301, 2013.

[24] P. Burgholzer, G. J. Matt, M. Haltmeier, and G. Paltauf, "Exact and approximative imaging methods for photoacoustic tomography using an arbitrary detection surface," *Phys. Rev. E*, vol. 75, p. 046706, 2007.